JOURNAL OF MATERIALS SCIENCE 22 (1987) 3685–3692

Humidity sensors using KH_2PO_4-doped porous (Pb, La)(Zr, Ti)O_3

Y. SADAOKA, M. MATSUGUCHI, Y. SAKAI
Department of Industrial Chemistry, Faculty of Engineering, Ehime University, Matsuyama 790, Japan

H. AONO
Department of Industrial Chemistry, Niihama National College of Technology, Niihama 792, Japan

S. NAKAYAMA, H. KUROSHIMA
Research and Development Center, Fine Ceramic Division, Shinagawa Refractories Co. Ltd, Bizen 705, Japan

Humidity sensing devices were prepared by using fine porous (Pb, La) (Zr, Ti)O_3 (PLZT) particles with ferroelectricity instead of insulating metal oxides such as alumina and zircon. The impedance of PLZT with 1 wt%. KH_2PO_4 was $10^6\,\Omega$ and lower than that of zircon with 3.8 wt% KH_2PO_4 by a factor of 10^2 in a dry atmosphere. In addition, the impedance in a humid atmosphere was controlled by the adding of potassium dihydrogen phosphate and changed by about four orders of magnitude in the humidity region 0 to 90% relative humidity at 1 kHz for samples burnt at 700° C. The humidity dependence of impedance is mainly governed by the change of coverage of adsorbed water. The hydrophilicity is affected by the burning temperature and lanthanum content of PLZT used as starting particle for porous PLZT ceramics burnt with KH_2PO_4. From complex impedance analysis it is confirmed that the resistive component inserted in parallel with the capacitive component decreases steeply with an increase in humidity, while the capacitive component is poorly dependent on the humidity.

1. Introduction

In general, the admittance of insulating porous ceramics such as alumina and zircon without any mobile charge carriers is enhanced by the formation of a physisorbed water layer on the particle surfaces; the self-dissociated proton of physisorbed water acts as the charge carrier and the proton can migrate in the physisorbed water layer [1–3]. The admittance in a humid atmosphere is characterized by the coverage of physisorbed water and the surface area and/or the microstructure of the porous ceramics [4, 5].

Porous oxide is a material adequate for a conventional humidity sensing device. However, most of the usual ceramic sensors are insulators, so that the impedance is $10^8\,\Omega$ cm or more in the low-humidity region and it is difficult to detect humidity changes by using a conventional impedance meter. In order to overcome this disadvantage, doping with a mobile cation such as proton, lithium, sodium and potassium into porous ceramics [6–8] and the formation of a superionic conductor [9] have been considered. In the former cases it is difficult to decrease the impedance in the low-humidity region, while the impedance in a humid atmosphere is easily controlled. In the latter case a decrease in the impedance over the whole humidity region is easily achieved, while it is difficult to obtain porous ceramics in which the microstructure and homogeneities are well controlled.

In a previous paper [10] it has been reported that sintered ferroelectric ceramics with potassium dihydrogen phosphate (KH_2PO_4) are superior with respect to the response time and sensitivity, i.e. the impedance is 10^6 to $10^7\,\Omega$ cm in the low-humidity region and changes by 3 to 4 orders of magnitude in region 0 to 90% relative humidity. In addition, it was reported that the impedance of burnt zircon with alkali phosphate is lower than that of burnt zircon with phosphoric acid in a humid atmosphere [6] and the humidity–impedance characteristic is preferable in respect of durability and reproducibility [7].

This paper presents the results of the humidity dependence of impedance and the influences of the amount of doped KH_2PO_4 and the heat treatment temperature on humidity sensitivity.

2. Experimental procedure

PbO, La_2O_3, ZrO_2 and TiO_2 were weighed in the prescribed mole ratio and mixed. $Pb_{1-x}La_x(Zr_yTi_{1-y})_{1-0.25x}O_3$ powder made by calcining the corresponding mixture at 900° C for 2 h was pulverized with ethanol for 2 h in a vibrating mill with ZrO_2 balls, and dried. The powder obtained was pressed under $1000\,kg\,cm^{-2}$ and sintered under an oxygen atmosphere at 1050 to 1150° C for 40 h. The ceramic thus obtained (PLZT) was pulverized by using the vibrating mill. The PLZT powder and potassium dihydrogen

0022–2461/87 $03.00 + .12

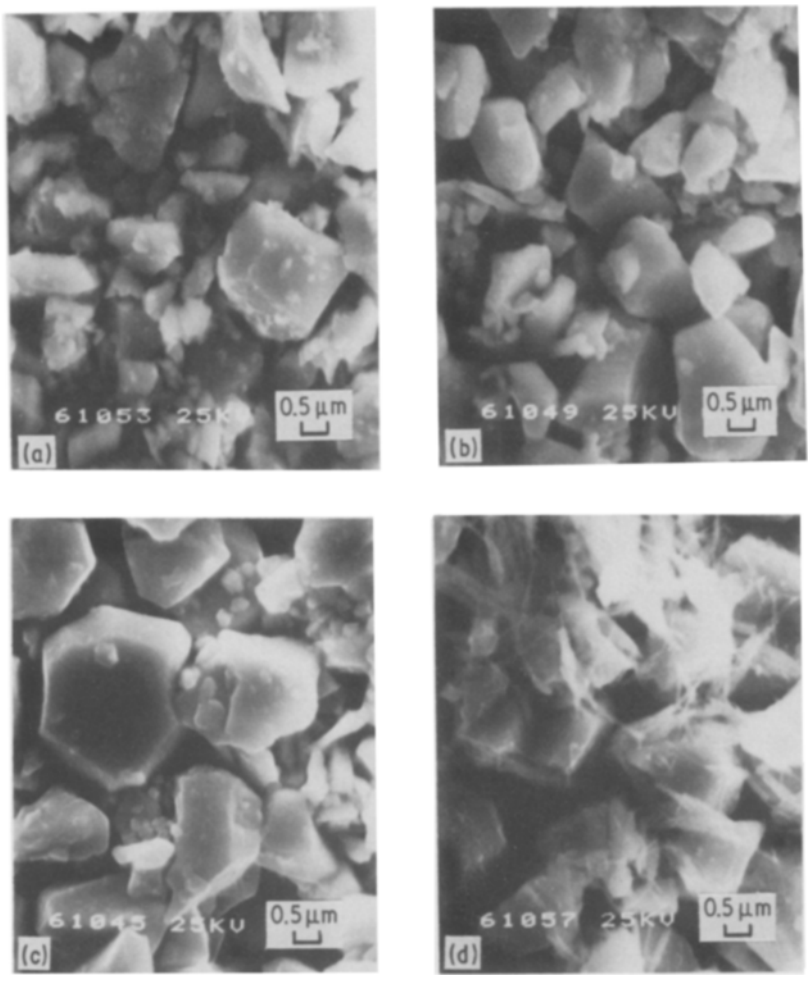

Figure 1 Scanning electron micrographs. (a) PLZT/0.09/0.65/0.1/700, (b) PLZT/0.09/0.65/0.5/700, (c) PLZT/0.09/0.65/1/700, (d) PLZT/0.09/0.65/5/700.

phosphate were weighed in the prescribed weight ratio and mixed with water as a mixing medium.

Sandwich-type elements were prepared as follows: first the prepared slurry was slowly dried at 100° C and pulverized, secondly the powder was pressed into a disc at 400 kg cm^{-2} and the disc was then shaped to 10 mm × 10 mm. The disc with ca. 0.5 mm thickness was burnt at some temperature in air for 3 h. Next, gold electrodes, 4 mm × 4 mm, were applied to opposite faces of the disc by a vacuum evaporation method.

TABLE I Average particle diameters of PLZT particles and surface areas of burnt ceramics

Sample	Burning temperature (° C)	Average particle diameter (μm)	Surface area (m^2 g^{-1})
PLZT/0.09/0.65/0.1	700	3.0	1.24
	1000	3.0	0.56
PLZT/0.09/0.65/0.5	700	3.0	1.47
	1000	3.0	0.46
PLZT/0.09/0.65/1.0	700	3.0	1.42
	1000	3.0	0.45
PLZT/0.09/0.65/5.0	700	3.0	1.11
	1000	3.0	0.25
PLZT/0.01/0.65/1.0	700	3.1	0.52
PLZT/0.03/0.90/1.0	700	1.2	0.98
PLZT/0.15/0.40/1.0	700	2.5	0.54
PLZT/0.20/0.65/1.0	700	1.8	1.40
PLZT/0.23/0.10/1.0	700	1.6	0.70
PLZT/0.00/0.35/1.0	700	2.0	0.46
PLZT/0.00/0.65/1.0	700	2.7	0.47

Humidity–impedance characteristics were measured with impedance meters (10^2 to 10^6 Hz). Relative humidities (r.h.) ranging from 0 to 90% were prepared by mixing dry and moist air in controlled proportions in the temperature range 30 to 45° C. The microstructure and the pore size distribution were examined by means of scanning electron microscopy and mercury penetration porosimetry, respectively. The surface area was determined by the BET method with nitrogen gas as a sorbate. The adsorption isotherm for H_2O was obtained by the gravimetric method.

3. Results

3.1. Microstructure and related characteristics

In Table I, the average particle diameters of the starting PLZT particles and the surface areas of burnt ceramics with potassium dihydrogen phosphate are summarized with the values of x, y and the weight percentage of KH_2PO_4. Hereafter, a specimen of $Pb_{1-x}La_x(Zr_yTi_{1-y})_{1-0.25x}O_3$ with w wt% KH_2PO_4 burnt at T° C will be referred to as PLZT/x/y/w/T.

Fig. 1 shows the surface microstructure of specimens burnt at 700° C observed by scanning electron microscopy (SEM). All specimens showed a porous microstructure. The nuclei of the observed particles consist of the main component, PLZT, and it is considered that potassium dihydrogen phosphate exists on the surface of the PLZT particles. In addition, it was confirmed that new needle-like crystals appeared on the surface of particles for PLZT/0.09/0.65/5/700, while needle-like crystals were not observed for

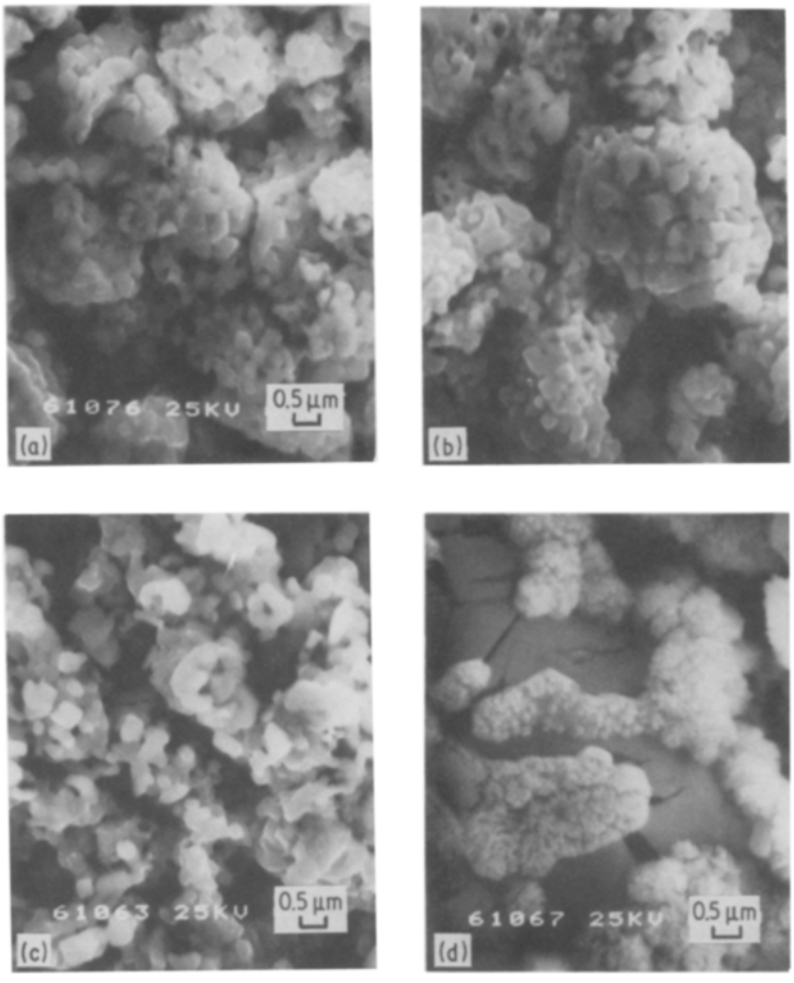

Figure 2 Scanning electron micrographs. (a) PLZT/0.09/0.65/0.1/1000, (b) PLZT/0.09/0.65/0.5/1000, (c) PLZT/0.09/0.65/1/1000. (d) PLZT/0.09/0.65/5/1000.

PLZT/0.09/0.65/w/700 ($w \leqq 1$). Fig. 2 shows the surface microstructure of specimens burnt at 1000° C. By comparing with Fig. 1, it was clear that the form of the particles was very different from that of the specimens burnt at 700° C. For specimens in which the concentration of potassium dihydrogen phosphate was less than 2 wt %, the existence of fine particles was confirmed on PLZT particles and the form of some PLZT particles was changed. For PLZT/0.09/0.65/5/1000, sintered PLZT and the formation of sponge-like phases were confirmed, while a surface analysis was not done. In standard X-ray diffraction results, all the signals assigned to PLZT for PLZT/0.09/0.65/w/700 ($w \leqq 1$) and for PLZT/0.90/0.65/5/700 and PLZT/0.09/0.65/10/1000, some new weak signals which could not be assigned to PLZT were observed.

The pore-size distribution of specimens was determined by mercury penetration porosimetry. The average pore radius and pore volume were estimated to be 0.1 to 0.4 μm and 0.03 to 0.04 $cm^3\ g^{-1}$, respectively. The pore volume decreased slightly with an increasing amount of doped KH_2PO_4 and the average pore radius increased with an increase in burning temperature.

From these observed results, it is considered that PLZT/0.09/0.65/w/700 ($w \leqq 1$) is a suitable ceramic for making humidity sensors in which the microstructure and homogeneities are well controlled.

3.2. Water adsorption isotherms

In Fig. 3, the relationship between the coverage of adsorbed water and humidity is shown. The coverage for PLZT with low contents of lanthanum was considerably larger than that for PLZT with high contents of lanthanum, especially in the high-humidity region, while the surface area of these samples was poorly dependent on the composition of the PLZT particles used as a starting material.

For PLZT/0.09/0.65/w/700 ($0.1 \leqq w \leqq 5.0$), although the surface area (S_{N_2}) determined by the BET method was poorly dependent on the concentration of potassium dihydrogen phosphate as an additive (Table I), the amount of adsorbed water

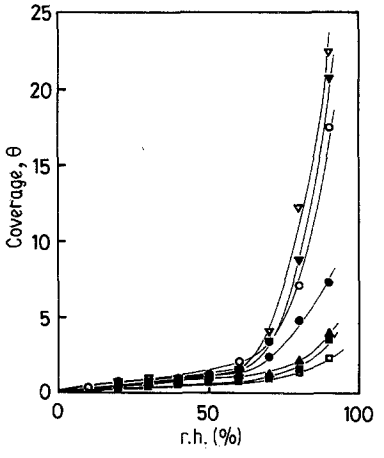

Figure 3 Humidity dependence of coverage of physisorbed water. (▼) PLZT/0.00/0.65/1/700, (▽) PLZT/0.00/0.35/1/700, (○) PLZT/0.01/0.65/1/700, (●) PLZT/0.03/0.90/1/700, (▲) PLZT/0.15/0.40/1700, (□) PLZT/0.20/0.65/1/700, (■) PLZT/0.23/0.10/1/700.

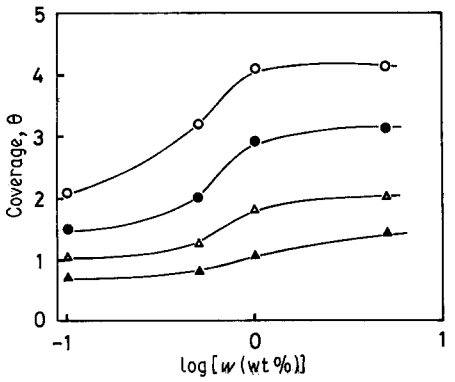

Figure 4 Relationship between coverage and content of KH_2PO_4 for PLZT/0.09/0.65/w/700. (▲) 40% r.h., (△) 60% r.h., (○) 80% r.h., (●) 90% r.h.

increased with an increasing concentration of potassium dihydrogen phosphate. The coverage (θ) of adsorbed water can be estimated from the value of the surface area and the amount of adsorbed water. Fig. 4 shows the relationship between the coverage at each humidity and the amount of potassium dihydrogen phosphate in wt %. In the lower-content region the coverage increases with increasing amount of potassium dihydrogen phosphate, and this dependency was lowered in the high-content region above 1 wt %. For the sample PLZT/0.09/0.65/1/700 the surface concentration of potassium dihydrogen phosphate is estimated to be about 40 molecules per nm^2. It seems that all of the surfaces of PLZT particles are covered by potassium dihydrogen phosphate for samples with 1 wt % or more of potassium dihydrogen phosphate. On the other hand, for PLZT/0.09/0.65/w/1000 ($w \geqq 1$) the relationship between the coverage and the humidity differed from the results for PLZT/0.09/0.65/w/700, i.e. the coverage for PLZT/0.09/0.65/5/T increased over the whole humidity range by raising the burning temperature up to 1000° C, and the reverse tendency was observed for PLZT/0.09/0.65/1/T as shown in Fig. 5. These observed results convinced us of the difference of surface structure as shown in Figs 1 and 2.

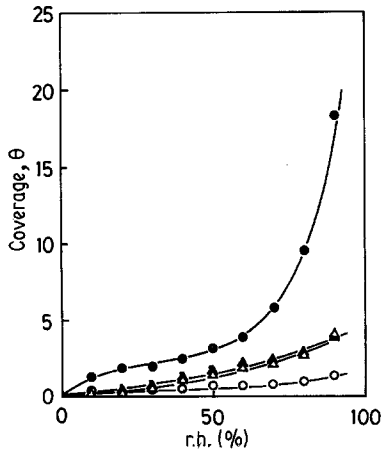

Figure 5 Humidity dependence of coverage of physisorbed water. (△) PLZT/0.09/0.65/1/700, (▲) PLZT/0.09/0.65/5/700, (○) PLZT/0.09/0.65/1/1000, (●) PLZT/0.09/0.65/5/1000.

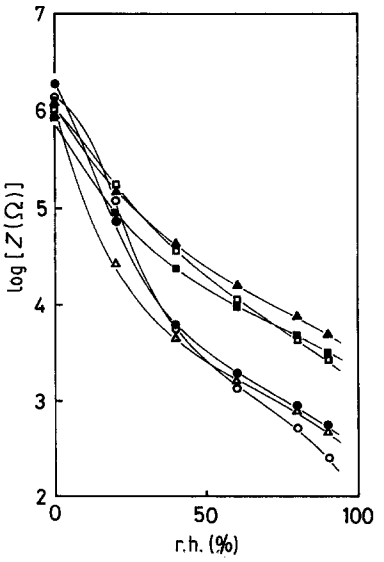

Figure 6 Humidity dependence of impedance measured at 1 kHz and 30° C. (○) PLZT/0.01/0.65/1/700, (●) PLZT/0.03/0.90/1/700, (△) PLZT/0.09/0.65/1/700, (▲) PLZT/0.15/0.40/1/700, (□) PLZT/0.20/0.65/1/700, (■) PLZT/0.23/0.65/1/700.

3.3. Humidity dependence of impedance

Fig. 6 shows the humidity–impedance relationships for some PLZTs with 1 wt % of KH_2PO_4 burnt at 700° C. In a dry atmosphere, the impedance observed at 1 kHz was poorly dependent on the composition of PLZT particle, while it was confirmed that the impedance in a humid atmosphere was affected by the composition of PLZT, i.e. the impedance for PLZT with lower contents of lanthanum was considerably lower than that for PLZT with higher contents of lanthanum. These differences are interpretable in terms of the difference of the coverage of adsorbed water, since the surface area is almost independent of the composition.

Fig. 7 shows the humidity–impedance characteristics

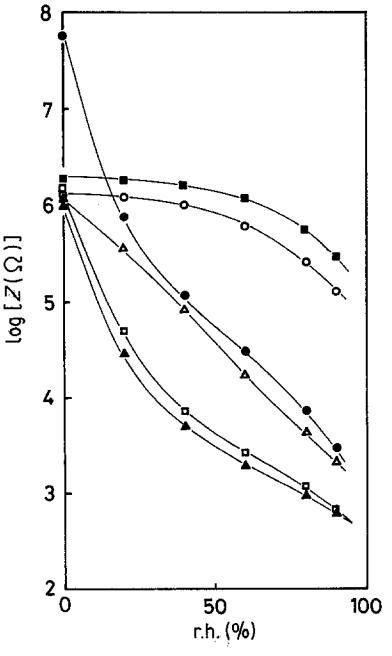

Figure 7 Humidity dependence of impedance measured at 1 kHz and 30° C. (○) PLZT/0.09/0.65/0.1/700, (△) PLZT/0.09/0.65/0.5/700, (▲) PLZT/0.09/0.65/1.0/700, (□) PLZT/0.09/0.65/5.0/700, (●) zircon with 3.8 wt % KH_2PO_4 burnt at 700° C.

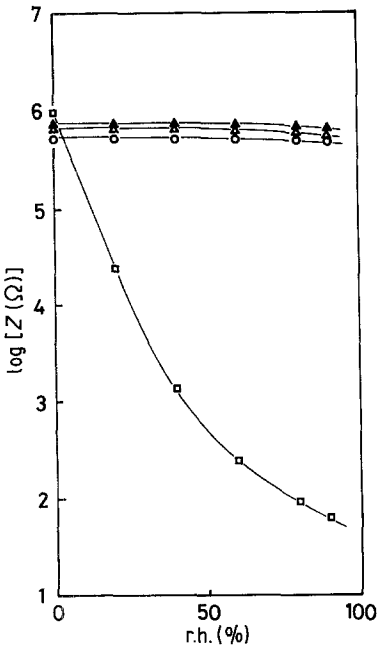

Figure 8 Humidity dependence of impedance measured at 1 kHz and 30° C. (○) PLZT/0.09/0.65/0.1/1000, (△) PLZT/0.09/0.65/0.5/1000, (▲) PLZT/0.09/0.65/1.0/1000, (□) PLZT/0.09/0.65/5.0/1000.

at 1 kHz and 30° C for PLZT without KH_2PO_4, PLZT with KH_2PO_4 and zircon ($ZrSiO_4$) with 3.8 wt % of KH_2PO_4. For zircon with KH_2PO_4 the impedance in the region 0 to 90% r.h. changed by about four orders of magnitude (10^8 to $10^3\,\Omega$). On the other hand, the impedance of PLZT without KH_2PO_4 in 0% r.h. showed $2 \times 10^6\,\Omega$ and was considerably lower than that for zircon-based ceramics, while the impedance in the region 0 to 90% r.h. changed by only about one order of magnitude. In specimens of PLZT burnt with KH_2PO_4 the impedance in a dry atmosphere was 1×10^6 to $2 \times 10^6\,\Omega$ and changed by about three orders of magnitude over the whole humidity region. In a humid atmosphere, the impedance decreased with an increase in the amount of KH_2PO_4 additive.

In Fig. 8, the impedance–humidity characteristics for PLZT with KH_2PO_4 burnt at 1000° C are shown. For samples in which the concentration of KH_2PO_4 was less than 2 wt %, no distinct variation of impedance with humidity was observed, while for PLZT with 5 wt % KH_2PO_4 the impedance changed by about

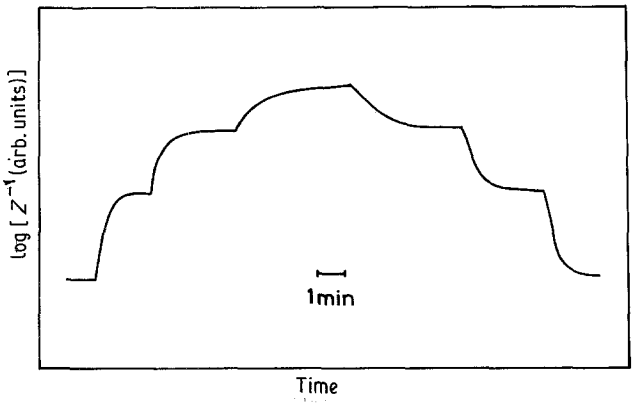

Figure 9 Impedance response for humidity changes from 10% r.h. to 90% r.h. step by step (10–30–60–90% r.h.) and vice versa for PLZT/0.09/0.65/1/700.

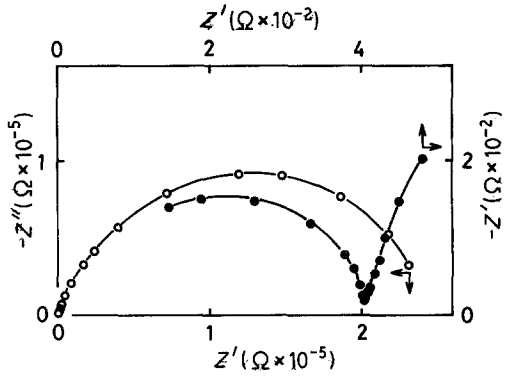

Figure 10 Complex impedance plots for PLZT/0.09/0.65/1/700. (○) 20% r.h., (●) 90% r.h.

four orders of magnitude over the whole humidity region. Thus the observed effect of the concentration of KH_2PO_4 on the humidity–impedance characteristics may be attributed to variations in the form and structure of the ceramic body as shown in Figs 1 and 2, and to differences in the hydrophilicity (Fig. 5).

In Fig. 9, the impedance responses for stepwise humidity changes from 10 to 90% r.h. and vice versa are shown for PLZT/0.09/0.65/1/700. By using the method of mixing dry and moist air a stationary humidity was achieved within 2 min after setting a certain humidity. It is clear that a stationary value of impedance is observed within about 2 min except at 90% r.h., and no distinct hysteresis is detected.

3.4. Complex impedance analysis

It is well known that impedance may be expressed by an appropriate equivalent circuit composed of resistive and capacitive components. These components can be estimated from a complex impedance analysis. Some typical complex impedance plots are shown in Fig. 10. In the high-frequency region the complex impedance plots were expressed as semicircles having one intersection with the real axis at the origin of the axis. From these results it is clear that the frequency dependence of impedance can be expressed by the equivalent circuit shown in Fig. 11. Fig. 12 shows the relationship between the logarithm of R_P and the humidity for PLZT/0.09/0.65/5/700. The value of R_P decreased steeply with increase in humidity, while C_P was scarcely dependent on humidity and the estimated value of the dielectric constant was about 2×10^3. It is therefore concluded that the impedance variation with humidity is caused by a variation of the resistive component. In addition, it was confirmed that the resistive component decreased with an increase in operating temperature, but no distinct temperature dependence of the capacitive component was detected as shown in Fig. 12.

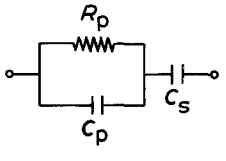

Figure 11 Equivalent circuit. C_P and C_s refer to the capacitance, R_P refer to the resistance.

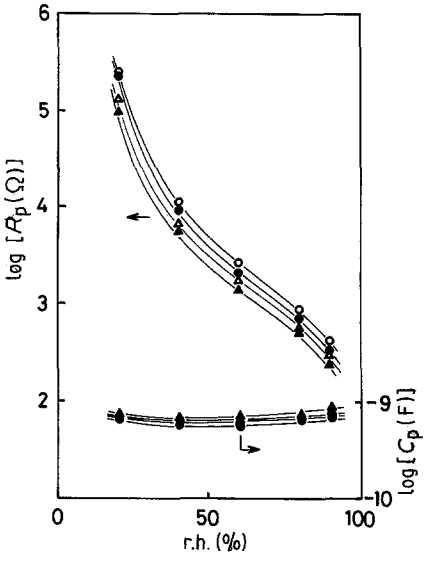

Figure 12 Humidity dependence of R_P and C_P for PLZT/0.09/0.65/1/700. (○) 30° C, (●) 35° C, (△) 40° C, (▲) 45° C.

4. Discussion

4.1. Humidity dependence of impedance

It is well known that the admittance of a porous ceramic without any mobile carriers is usually enhanced by the adsorption of water and/or capillary condensation of water [1, 2, 11, 12]. When water molecules are present on the surface of a porous ceramic but the surface coverage is not complete, H_3O^+ diffusion and H^+ hopping and/or transfer occur. When water molecules are abundant, the physisorbed water dissociates due to the high electrostatic field in the chemisorbed water:

$$2H_2O \rightarrow H_3O^+ + OH^-$$

Charge transport occurs when the hydronium ion releases a proton to a neighbouring water molecule (Grotthuss chain reaction). In these cases, it is expected that the admittance in a humid atmosphere is proportional to the surface area and the amount of adsorbed water under conditions where the coverage of physisorbed water is larger than 2(4.6) and all the pores consist of through-pores without closed and accessible pores (in this case, the effect of tortuosity of pores is ignored for simplicity). If proton transport is governed by the jump probability of a proton into trapping and/or hopping sites, the jump frequency (ω_J) depends upon the potential barrier expressed by

$$\omega_J = v_0 \exp(\Delta S/k) \exp(-\Delta H/kT) \quad (1)$$

where v_0 is the vibrational frequency for a carrier, ΔS is the entropy of migration and ΔH is the enthalpy of migration. For this system, the adsorbed water should act to provide trapping and/or hopping sites for the mobile protons.

Finally, the conductivity (σ) is given by

$$\sigma = na^2e^2\omega_J/kT \quad (2)$$

where a is the jump distance, e is the elementary charge and n is the carrier concentration. As mentioned above, the observed impedance consists of capacitive and resistive components and the resistive component is strongly dependent on the operating

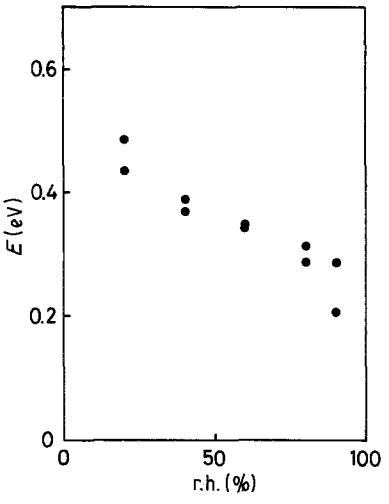

Figure 13 Humidity dependence of activation energy for PLZT/0.09/0.65/1/700.

temperature and the humidity, while the capacitive component is not. It is confirmed that the temperature dependence of the resistive component (R_P) estimated from the complex impedance analysis as expressed by

$$R_P = R_0 \exp(-E/kT_0) \exp(E/kT) \quad (3)$$

where R_0 is the pre-exponential factor which is inversely proportional to the carrier concentration and its mobility, E is the activation energy, k is the Boltzmann constant, T is the absolute temperature and T_0 is a characteristic constant. According to the hopping model, the pre-exponential term is a function of the carrier concentration and the hopping attempt frequency between sites separated by a given distance, i.e.

$$R_0^{-1} = na^2e^2v_0/kT \quad (4)$$

In this case an activation entropy term is involved in the exp $(-E/kT_0)$ term in Equation 3. Figs 13 and 14 show the humidity dependence of the activation energy in the resistive component at each relative humidity and the relationship between the activation energy and the resistive component at 30° C, respectively.

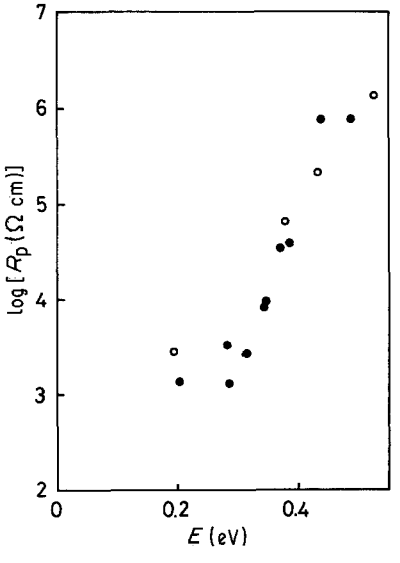

Figure 14 Relationship between resistivity at 30° C and its activation energy. (●) PLZT/0.09/0.65/1/700, (○) zircon with 3.8 wt % KH_2PO_4 burnt at 700° C.

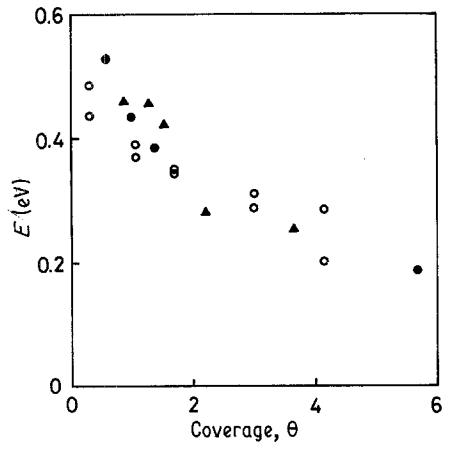

Figure 15 Relationship between activation energy and coverage of physisorbed water. (○) PLZT/0.09/0.65/1/700, (▲) zircon with 3.8 wt% KH_2PO_4 burnt at 700° C, (●) zircon with 3.8 wt% NaH_2PO_4 burnt at 700° C.

It is clear that the activation energy decreases monotonously with an increase in humidity and the logarithm of the resistive component increases with an increase in the activation energy. For comparison, the relationship between the logarithm of R_P and its activation energy for burnt zircon with 3.8 wt% XH_2PO_4 (X = Na, K) is shown in Fig. 14. No distinct differences were observed between the results obtained for burnt zircon with 3.8 wt% XH_2PO_4 and PLZT/0.09/0.65/5/700.

In the previous paper [6], the activation energy of resistance for zircon burnt with XH_2PO_4 (X = H, Na, K) was found to be a function of the coverage of physisorbed water and poorly dependent on the X species. Fig. 15 shows the relationship between the activation energy and the coverage of physisorbed water, with the results obtained for burnt zircon with XH_2PO_4. While in the lower-coverage region the activation energy observed in PLZT/0.09/0.65/5/700 is slightly lower than that of burnt zircon with XH_2PO_4, a fair agreement between the two systems is confirmed. Thus the results indicate that the resistive component is mainly governed by the existence of KH_2PO_4, and the humidity dependence of the resistive component is interpretable in terms of a decrease in the activation energy with the coverage of physisorbed water. It may be considered that the discrepancies observed in the lower-coverage region are caused by the difference of the dielectric constant of the nucleus particle (the dielectric constant of PLZT (2000) is much higher than that of zircon (~ 10)), since the dissociation energy of a carrier decreases with the dielectric constant of the medium [2], but at the present time it is difficult to discuss this in more detail. If this presumption is correct, the activation energy term in Equation 3 must involve the activation energy of dissociation of adsorbed water, especially in the lower-coverage region.

4.2. Effects of KH_2PO_4 and burning temperature on the impedance–humidity relationship

As shown in Figs 1 and 2, for PLZT/0.09/0.65/w/700 ($w \leqq 1$), the particle form resembles that of the starting particles of PLZT. This means that most of the KH_2PO_4 exists on PLZT particles. The surface concentration of potassium dihydrogen phosphate is estimated to be about 40 molecule per nm^2 for PLZT/0.09/0.65/1/700 (it seems that the cross-sectional surface area of phosphate is about 0.1 nm^2) by assuming that no reactions occur between potassium dihydrogen phosphate and the PLZT particles. The amount of adsorbed water increased with an increase in KH_2PO_4 additive up to $w = 1$ and was poorly dependent on the concentration of the additive in the region above $w = 1$, as shown in Fig. 3. The addition of an excess amount of KH_2PO_4 is responsible for the formation of needle-like KH_2PO_4.

For PLZT/0.09/0.65/w/1000 ($w \leqq 1$), the form was very different from the starting particle one, i.e. the surface of the nucleus was covered by small sintered particles. In addition, the average pore radius determined by mercury penetration porosimetry increased and the surface area decreased by raising the burning temperature up to 1000° C as listed in Table I. For PLZT/0.09/0.65/5/1000, the form of the body was different to other samples as shown in Figs 1 and 2 i.e. sintered particles with some cracks and new clusters composed of small particles were observed. It seems that the former are mainly composed of PLZT and the latter of KH_2PO_4, although an elemental analysis was not done.

The water adsorption isotherm was strongly affected by the burning temperature. As shown in Fig. 5, the humidity dependence of the coverage of adsorbed water for PLZT/0.09/0.65/w/700 ($w = 1.5$) was poorly dependent on w, but the relationship was strongly dependent on w, i.e. the coverage decreased for PLZT/0.09/0.65/1/1000 and increased for PLZT/0.09/0.65/5/1000 by raising the burning temperature up to 1000° C. It seems that for PLZT/0.09/0.65/w/1000 ($w \leqq 1$), most of the KH_2PO_4 reacts with PLZT and the surface is covered by newly reacted material, since

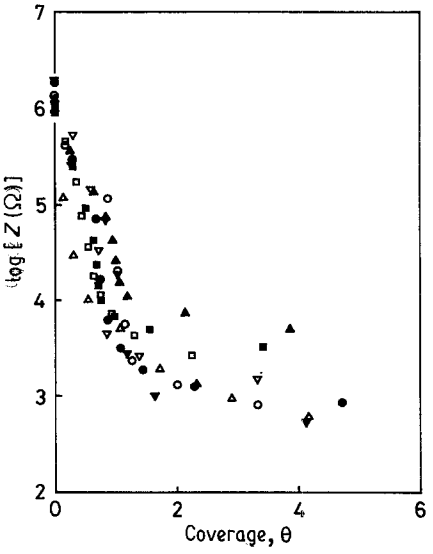

Figure 16 Relationship between impedance and coverage of physisorbed water for PLZT with 1 wt% KH_2PO_4 burnt at 700° C. (▼) PLZT/0.00/0.65/1/700, (▽) PLZT/0.00/0.35/1/700, (○) PLZT/0.01/0.65/1/700, (●) PLZT/0.03/0.90/1/700, (▲) PLZT/0.15/0.40/1/700, (□) PLZT/0.20/0.65/1/700, (■) PLZT/0.23/0.10/1/700.

the hydrophilic nature is very different to that for PLZT/0.09/0.65/w/700. By comparing the results of impedance–humidity relationships, it was confirmed that the impedance for PLZT/0.09/0.65/w/700 was strongly affected by humidity, but no distinct dependencies were observed for PLZT/0.09/0.65/w/1000 ($w \leqq 1$). Since in log–log plots of impedance and applied frequency the slope of the line for PLZT/0.09/0.65/1/1000 is nearly equal to -1 in the whole frequency and humidity range, the impedance is approximately equal to the capacitive component and poorly dependent on humidity, and the resistive component is very high. As the origin of these differences, hydrophilicity of the particle surface is considered (Fig. 5), since the difference of surface area was not so much as listed in Table I and the resistivity of the element prepared at 700° C was lower than that of the element prepared at 1000° C by a factor of 10^4 or more at 90% r.h. In addition, for PLZT/0.09/0.65/5/1000 the appearance of humidity dependency of impedance is brought about by an increase in hydrophilicity (Fig. 5).

4.3. Effect of composition of PLZT on impedance–humidity relationship

The impedance–humidity relationships and water adsorption isotherms were strongly affected by the composition of the PLZT used as starting material. To examine the effect of composition on these characteristics, some PLZT particles were prepared with similar particle diameters as listed in Table I. In Fig. 3, the relationship between the coverage of adsorbed water and humidity is shown. The coverage of water was poorly dependent on the composition of PLZT in the lower-humidity region, but that for PLZT with low contents of lanthanum was considerably larger than that for PLZT with high contents of lanthanum, in the higher humidity region. In general, it seems that the hydrophilicity increases with an increase in the content of lanthanum, but the observed results show the reverse tendencies. As one of the causes, the difference of pore size distribution is considered. According to the capillary condensation model for water, water condensation occurs in pores with a diameter below about 20 nm at 90% r.h. and 20° C. However, the existence of such small pores may be contradicted, since the surface area determined by the BET method with N_2 (cross-sectional area of molecule 0.162 nm^2) is scarcely dependent on the composition of PLZT. In addition, the surface concentration of potassium dihydrogen phosphate is estimated to be 40 to 100 molecule per nm^2 and this concentration is enough to cover the whole of the particle surface of PLZT. If the whole of the surface is covered by KH_2PO_4 and no reactions between KH_2PO_4 and PLZT proceed, it is expected that the humidity dependence of the coverage of water will be independent of the composition of PLZT. But as shown in Fig. 3, the hydrophilicity is affected by the content of lanthanum, so it seems that KH_2PO_4 reacts with PLZT and this reactivity depends on the composition of PLZT. As mentioned above (section 4.1), the resistance in a humid atmosphere is expressed by Equation 3 and the variation of resistance is mainly caused by the changes of activation energy with humidity rather than by changes of the R_0 component. In addition, the activation energy is expressed as a function of the coverage of physisorbed water. These relationships suggest that the resistance (impedance) is expressed as a function of the coverage of physisorbed water, since the impedance is approximated by the resistance in a humid atmosphere. This prediction is confirmed in PLZT with 1 wt% of KH_2PO_4 burnt at 700° C, while some variations from sample to sample are perceived as shown in Fig. 16.

Further detailed results relating to the composition of the surface and the reactivities of PLZT and alkali phosphate will appear in the near future.

References

1. J. J. FRIPIAT, A. JELLI, G. PONCELET and J. ANDRÉ, *J. Phys. Chem.* **69** (1965) 2185.
2. J. H. ANDERSON and G. A. PARKS, *ibid.* **72** (1968) 3662.
3. G. CLEMENT, H. KNÖZINGER, W. STÄHLIN and B. STÜBNER, *ibid.* **83** (1979) 1280.
4. Y. SADAOKA and Y. SAKAI, *Denki Kagaku* **51** (1983) 879.
5. *Idem, ibid.* **51** (1983) 873.
6. *Idem, J. Mater. Sci. Lett.* **5** (1986) 656.
7. *Idem,* in Proceedings of the 2nd International Meeting on Chemical Sensors, Bordeaux (Bordeaux Chemical Sensors, Bordeaux, 1986) p. 357.
8. F. UCHIKAWA and K. SHIMAMOTO, *Amer. Ceram. Soc. Bull.* **64** (1985) 1137.
9. Y. SADAOKA and Y. SAKAI, *J. Mater. Sci.* **20** (1985) 3027.
10. Y. SADAOKA, H. AONO, Y. SAKAI, S. NAKAYAMA and H. KUROSHIMA, *J. Mater. Sci. Lett.* **5** (1986) 923.
11. Y. SHIMIZU, H. ARAI and T. SEIYAMA, *Sensors and Actuators* **7** (1985) 11.
12. Y. SADAOKA, Y. SAKAI and S. MATSUMOTO, *J. Mater. Sci.* **21** (1986) 1269.

Received 18 November 1986
and accepted 29 January 1987